Analysis of sensitivity and optimization for mistuned bladed disk forced response using high-fidelity models

Article (Accepted Version)

Analysis of Sensitivity and Optimization for Mistuned Bladed Disk Forced Response Using High-Fidelity Models

Yuanqiu Tan[a], Chaoping Zang[a], E.P. Petrov[b]

[a] Nanjing University of Aeronautics and Astronautics , Jiangsu Province Key Laboratory of Aerospace Power System, Nanjing 210016, China, y.tan@nuaa.edu.cn; e-mail: c.zang@nuaa.edu.cn
[b]University of Sussex, Brighton BN1 9QT, United Kingdom, e-mail: y.petrov@sussex.ac.uk

ABSTRACT

An effective method is developed for efficient calculations of the sensitivity of the maximum forced response levels for mistuned bladed disks with respect to blade frequency mistuning. The expressions for 1st and 2nd order sensitivity coefficients are derived in an analytical form which provides high accuracy and computational efficiency. Then, the optimization methods are used for searching the best and worst mistuning patterns of bladed disks. Two major types of the mistuning optimization problems are considered: (i) a continuous optimization problem when the blade mistuning can take any values from a prescribed range and (ii) a combinatorial optimization problem, when the set of mistuned blades is given and the optimization can be achieved by blade re-arrangement in a disk. For the first type of the optimization problem a set of sensitivity-based optimization algorithms is applied and for the second type a variant of a genetic algorithm is developed. The analysis of mistuning sensitivity coefficients and results of optimization searching are shown on an example of a realistic turbine bladed disk.

NOMENCLATURE

$\boldsymbol{K},\boldsymbol{M},\boldsymbol{C}$ - stiffness, mass and damping matrices of a tuned bladed disk

$\delta\boldsymbol{K},\delta\boldsymbol{M},\delta\boldsymbol{C}$ - deviations of stiffness, mass and damping matrices of a mistuned bladed disk from their tuned counterparts

$\delta\boldsymbol{M}_j$ and $\delta\boldsymbol{K}_j$ - deviations of stiffness and mass matrices for j-th blade

$\boldsymbol{f}$ - excitation force vector for a bladed disk

$\boldsymbol{f}^S$ - excitation force vector applied to one bladed disk sector

N_B - the total number of blades in a bladed disk

$\eta_r, \omega_r, \boldsymbol{\phi}_r$ - modal damping factor, natural frequency, and mode shape of r-th mode

$\boldsymbol{A}$ - forced response function (FRF) matrix

$\boldsymbol{u}_j$ - vector of complex amplitudes for j-th node

$\boldsymbol{u}$ - vector of complex amplitudes for the node and the excitation frequency where the displacement is maximum

a_j - maximum magnitude of the vector of displacements for j-th node

a - maximum magnitude of the displacement vector found over all blades in the frequency range of interest

ω^-,ω^+ - lower and higher bounds of the frequency range analysed

$\boldsymbol{\Phi}$ - a matrix of mode shapes of a mistuned bladed disk

$\boldsymbol{\Phi}_k$ - a matrix of mode shapes selected only for nodes of k-th sector

$\boldsymbol{b}$ - the vector of parameters describing bladed disk mistuning

$\delta\boldsymbol{M}^S$ - a reference mass mistuning matrix for a sector

μ - a multiplier for the reference mass mistuning matrix corresponding to blade frequency mistuning value

$\boldsymbol{x}$ - the vector of complex amplitudes of bladed disk DOFs

$\boldsymbol{x}' = \partial\boldsymbol{x}/\partial b_j$ and $\dot{\boldsymbol{x}}' = \partial^2\boldsymbol{x}/\partial b_j\partial b_k$ - 1st and 2nd order sensitivities of the complex amplitudes to mistuning

$\partial a/\partial b_j$ and $\partial^2 a/\partial b_j\,\partial b_k$ - 1st and 2nd order sensitivities of the maximum bladed disk response

1. INTRODUCTION

Blades in realistic bladed disks are inevitably mistuned, which usually caused by small imperfections due to blade manufacture tolerances, scatters in contact interfaces properties, wear during gas-turbine engine service, etc. The forced response levels of bladed disks are very sensitive to blade mistuning variations and response levels can be increased by several times even when the blade mistuning is restricted within small ranges accepted by gas-turbine engine practical industry (see Refs. [1] and [2]). There are comprehensive reviews of the causes, problems and studies of mistuned bladed disk forced response, which were published in different times (see Refs.[3]-[5]).

The theoretical limit of the maximum amplitude amplification factor due to mistuning was derived by Whitehead in Refs. [6] and [7], where the limit value is defined by the number of blades in a bladed disk: $\left(1+\sqrt{N_B}\right)/2$, where N_B is the number of blades of the bladed disk. Another useful analytically-derived estimate for the maximum factor was proposed in Ref. [8]. These limits give convenient estimates for the maximum forced response of mistuned bladed disks, but in most cases are too conservative and do not take into account the effects of many influential parameters, such as damping, blade mistuning ranges, excitation force frequency and excited mode shapes, etc., which can result in different amplification factor values. Because of this, there is significant interest in the development of the approaches for obtaining the maximum amplification factors which take into account the details of a bladed disk design and operating conditions. The optimization search of the best and worst mistuning patterns was first formulated as a continuous optimization problem based on gradient information in Ref. [9], where the beam blade models are used. This approach has been extended to realistic finite element models of bladed disks in Ref. [10]. The estimates of the maximum amplification factors were obtained based on simplified blade models using semi-analytical derivations, e.g. see Refs.[11]-[13]. Effects of intentional mistuning patterns on the forced response levels of bladed disks were studied in Refs.[14]-[17], where linear, harmonic, alternate and partial mistuning patterns were considered. Further developments of the optimization techniques for mistuning analysis were also made: see e.g. Refs.[18] and [19].

For the assessment of mistuning effects of realistic bladed disks gas-turbine industry requires use of the high-fidelity modelling and analysis methods. Moreover, the important additional characteristics of the mistuned forced response are the forced response sensitivity to small variations of the blade mistuning, which allow assessment of the forced response robustness and can be used in the creation of the surrogate mistuning models or in applying gradient-based optimization methods for search for the maximum amplification factors (see e.g. Ref. [20]). Some approaches for the calculations of sensitivity coefficients for mistuned bladed disks have been proposed in papers [9] and [10], where the sensitivity coefficients are calculated for the maximum forced response displacements of bladed disks with respect to blade frequency mistuning. The optimization search of best and worst arrangements of given sets of mistuned blades was formulated as a combinatorial optimization problem in Ref. [20]. However, the combinatorial optimization problem was solved here using rather simplified models.

In this paper an effective method is developed for the calculation of first and second order sensitivity coefficients of the maximum forced response displacements with respect to blade mistuning parameters. The gradient-based optimization algorithms are introduced to search for the best and worst mistuning patterns using realistic large-scale finite element models of bladed disks. The use of the sensitivity coefficients accelerates the speed of optimization by providing the best direction for each step of the iterative optimization search. In addition, the problem of searching for the best and worst arrangements in a bladed disk of a given set of mistuned blades is formulated and a genetic algorithm is employed to perform the combinatorial optimization. Numerical studies are carried out to explore the first and second order sensitivity coefficients for frequency ranges corresponding to different mode shapes and excitation orders and damping. Effectiveness of a set of different gradient-based continuous optimization methods is assessed and the search for the worst and best mistuning patterns is performed for different families of modes and damping. The combinatorial optimization problem is solved for search for the best and worst blade arrangements using high-fidelity realistic turbine bladed disk and the possibility of reducing forced response levels by the re-arrangements is explored. The sensitivity analysis and the search for worst and best mistuning patterns is performed not only for the first family of modes but also for excitation in higher frequencies ranges corresponding high blade mode shapes, which has not been done to date.

2. METHOD FOR THE FORCED RESPONSE SENSITIVITY ANALYSIS

2.1 Forced response calculation

The equation of motion of a mistuned bladed disk subjected to the engine-order excitation can be written in the following general form:

$$\left[\left(\boldsymbol{K}+\delta\boldsymbol{K}\right)+i\left(\boldsymbol{C}+\delta\boldsymbol{C}\right)-\omega^2\left(\boldsymbol{M}+\delta\boldsymbol{M}\right)\right]\boldsymbol{x}=\boldsymbol{f} \tag{1}$$

where $\tilde{\boldsymbol{K}}=\boldsymbol{K}+\delta\boldsymbol{K}$, $\tilde{\boldsymbol{C}}=\boldsymbol{C}+\delta\boldsymbol{C}$, and $\tilde{\boldsymbol{M}}=\boldsymbol{M}+\delta\boldsymbol{M}$ are stiffness, damping, and mass matrix of a mistuned bladed disk respectively which are expressed as a sum of the nominal tuned matrix and a perturbation matrix which models blade mistuning properties; $\boldsymbol{x}=\left\{\boldsymbol{x}_1,\boldsymbol{x}_2,...,\boldsymbol{x}_{N_B}\right\}^T$ is a vector of complex amplitudes for all degrees of freedom in the structure, combined from the vectors of complex amplitudes of bladed disk sectors, $\boldsymbol{x}_j$; ω is the excitation frequency. The bladed disk is subjected to engine order (EO) type excitation and the excitation force vector, $\boldsymbol{f}$, takes the following form:

$$\boldsymbol{f}=\left\{\boldsymbol{f}^S,e^{i\alpha k}\boldsymbol{f}^S,\cdots,e^{i\alpha k\left(N_B-1\right)}\boldsymbol{f}^S\right\}^T \tag{2}$$

where $\boldsymbol{f}^S$ is the force vector applied to a reference sector; N_B is the blade number of bladed disk; $\alpha=2\pi/N_B$ is the sector angle, k is the engine order; $i=\sqrt{-1}$.

The determination of the complex amplitudes directly from solution of Eq.(1) is not practical for mistuned bladed disks due to very large size of the matrices obtained for finite element (FE) models commonly used in the industrial applications for bladed disk modelling. The use of the forced response function (FRF) matrix allows the problem of large computational efforts required for the mistuned forced response analysis to be alleviated and the expression for the forced response amplitudes take the form:

$$\boldsymbol{x}=\left[\left(\boldsymbol{K}+\delta\boldsymbol{K}\right)+i\left(\boldsymbol{C}+\delta\boldsymbol{C}\right)-\omega^2\left(\boldsymbol{M}+\delta\boldsymbol{M}\right)\right]^{-1}\boldsymbol{f}=\boldsymbol{A}\boldsymbol{f} \tag{3}$$

where the FRF matrix, $\boldsymbol{A}$, is calculated using modal characteristics of a mistuned structure:

$$\boldsymbol{A}=\sum_{j=1}^{m}\frac{\boldsymbol{\phi}_j\boldsymbol{\phi}_j^T}{(1+i\eta_j)\omega_j^2-\omega^2} \tag{4}$$

where η_j , ω_j , and $\boldsymbol{\phi}_j$ are modal damping factor, natural frequency, and corresponding mode shape, respectively, for the j -th mode and m is the total number of modes used in the FRF matrix evaluation. The mode shapes of a mistuned bladed disk can be calculated for some cases directly using modern FE software, yet this still can require unacceptable computational expense for most of cases. Because of this, we use in this paper the effective reduced-order method for determination of mistuned bladed disk modal properties which is proposed in Ref.[21]. The forced response of a mistuned structure can be effectively calculated by using the concept of modal excitation forces:

$$\boldsymbol{x}=\boldsymbol{A}\boldsymbol{f}=\left(\sum_{j=1}^{m}\frac{\boldsymbol{\phi}_j\boldsymbol{\phi}_j^T}{(1+i\eta_j)\omega_j^2-\omega^2}\right)\boldsymbol{f}=\sum_{j=1}^{m}\frac{\boldsymbol{\phi}_j^T\boldsymbol{f}}{(1+i\eta_j)\omega_j^2-\omega^2}\boldsymbol{\phi}_j=\sum_{j=1}^{m}\frac{c_j}{(1+i\eta_j)\omega_j^2-\omega^2}\boldsymbol{\phi}_j \tag{5}$$

where $c_j=\boldsymbol{\phi}_j^T\boldsymbol{f}$ is the j -th modal force which is calculated for each mode involved in the FRF matrix. The modal forces are calculated only once, before the calculation of the forced response over the frequency range of interest. The forced response analysis requires the large number of frequency steps to capture the multitude of resonance peaks of a mistuned structure and the reduction of the computation time, achieved by this formulation, is significant. Further reduction of the computation efforts can be easily made in this formulation by calculating the complex amplitudes for only a subset of nodes which are needed for the analysis: this can be done simply by selecting in the final expression in Eq.(5) from the mode shape vectors, $\boldsymbol{\phi}_j$, the modal displacements for degrees of freedom (DOFs) where the amplitudes are need to be determined.

The complex amplitudes are calculated in Eq.(5) for each j -th node for coordinate components of a three-dimensional vector of displacements: $\boldsymbol{u}_j=\left\{u_{xj}^{\mathrm{Re}}+iu_{xj}^{\mathrm{Im}},u_{yj}^{\mathrm{Re}}+iu_{yj}^{\mathrm{Im}},u_{zj}^{\mathrm{Re}}+iu_{zj}^{\mathrm{Im}}\right\}^T$. In the assessment of the levels of vibration the value of the maximum magnitude of this vector is usually required. The phase shifts between *x, y* and *z* displacement components do not allow using the well-known expression for the vector magnitude as Euclidian norm: $\sqrt{u_x^2+u_y^2+u_z^2}$. The expression for the maximum vector magnitude when the vector components are complex numbers was derived in Ref.[9] and this expression takes the following form:

$$a_j=\max_{0\le t\le 2\pi/\omega}\left\|\boldsymbol{u}_j e^{i\omega t}\right\|=\sqrt{\frac{1}{2}\left(\bar{\boldsymbol{u}}_j^T\boldsymbol{u}_j+\left|\boldsymbol{u}_j^T\boldsymbol{u}_j\right|\right)} \tag{6}$$

where a_j is the maximum value of three-dimensional nodal displacement calculated for j-th node. Consequently, the maximum forced response displacement of a whole mistuned bladed disk is searched over the excitation frequency range and among all bladed disk nodes of interest:

$$a(\boldsymbol{b}) = \max_{\omega\in\left[\omega^-,\omega^+\right]} \max_{j\in V}\left(a_j\right) = \sqrt{\frac{1}{2}\left(\bar{\boldsymbol{u}}^T\boldsymbol{u} + \left|\boldsymbol{u}^T\boldsymbol{u}\right|\right)} \tag{7}$$

where a is the maximum displacement of a bladed disk; ω^- and ω^+ are the low and high bounds of the excitation frequency range analysed, V is the bladed disk domain analysed. Here $\boldsymbol{u}$ is the vector of complex amplitudes evaluated at the bladed disk node and at the excitation frequency where the maximum bladed disk forced response displacement is found. The maximum bladed disk displacement is determined by comparison of maximum displacements for all analysed nodes of the bladed disk for each excitation frequency. This search is performed for all frequencies within the frequency analysed. The frequency step used for the seeping the frequency is varied to allow efficient determination of the multitude resonance peaks, which are inherent for mistuned bladed disks.

The bladed disk maximum amplitudes are dependent on the blade mistuning and the bladed disk mistuning pattern can be characterised by a vector, $\boldsymbol{b} = \left\{b_1, b_2, \cdots, b_{N_B}\right\}^T$, of mistuning parameters, b_j, which describe the discrepancy of each j-th blade dynamic properties from a 'tuned' blade - the nominal blade which is manufactured perfectly in accordance to the design requirements. The choice of the mistuning parameters can be different, this choice is dependent on the way how blade mistuning is characterised, for example, the mistuning parameters can describe: (i) blade frequency mistuning (e.g. see Refs. [21] and [22]); (ii) blade material anisotropy orientation mistuning for bladed made of monocrystalline material (see. Ref.[23]), (iii) blade geometric shape mistuning (e.g. see. Ref.[24]) .

2.2 Sensitivity for complex nodal amplitudes: a general case

The method developed in this paper allows determining the 1st and 2nd order sensitivities of the amplitudes to bladed mistuning and it is based on fully analytical derivation of the expressions for the sensitivities. The sensitivities for nodal complex amplitudes are obtained by taking the first and second order derivatives of Eq.(1) with respect to the blade mistuning parameters:

$$\boldsymbol{x}' = -\left[\boldsymbol{K} + \delta\boldsymbol{K} + i\left(\boldsymbol{C} + \delta\boldsymbol{C}\right) - \omega^2\left(\boldsymbol{M} + \delta\boldsymbol{M}\right)\right]^{-1}\left(\delta\boldsymbol{K}' - \omega^2\delta\boldsymbol{M}'\right)\boldsymbol{x} = -\boldsymbol{A}\left(\delta\boldsymbol{K}' - \omega^2\delta\boldsymbol{M}'\right)\boldsymbol{x} \tag{8}$$

$$\dot{\boldsymbol{x}}' = -\boldsymbol{A}\left[\left(\delta\dot{\boldsymbol{K}}' - \omega^2\delta\dot{\boldsymbol{M}}'\right)\boldsymbol{x} + \left(\delta\boldsymbol{K}' - \omega^2\delta\boldsymbol{M}'\right)\dot{\boldsymbol{x}} + \left(\delta\dot{\boldsymbol{K}} - \omega^2\delta\dot{\boldsymbol{M}}\right)\boldsymbol{x}'\right] \tag{9}$$

where the prime indicates here a derivative with respect to one of the chosen mistuning parameter, b_j, and dot corresponds to the derivative with respect to another mistuning parameter, b_k, e.g. $\boldsymbol{x}' = \partial\boldsymbol{x}/\partial b_j$ and $\dot{\boldsymbol{x}}' = \partial^2\boldsymbol{x}/\partial b_j\partial b_k$. Here, the FRF matrix takes into account the damping mistuning terms by using the modal damping factors provided for the mistuned modes in the equation for a mistuned bladed disk FRF matrix, given by Eq.(4), and the sensitivity of the forces response is determined with respect to mistuning parameters affecting the mass and stiffness matrices of a bladed disk. For a case considered here, the mistuning is introduced by mass mistuning matrix, $\delta\boldsymbol{M}$, and by stiffness mistuning matrix $\delta\boldsymbol{K}$ of all blades. The mass and stiffness mistuning matrices of a bladed disk takes the form:

$$\delta\boldsymbol{M} = diag(\delta\boldsymbol{M}_1, \delta\boldsymbol{M}_2, ..., \delta\boldsymbol{M}_{N_B}) \;\; ; \;\; \delta\boldsymbol{K} = diag(\delta\boldsymbol{K}_1, \delta\boldsymbol{K}_2, ..., \delta\boldsymbol{K}_{N_B}) \tag{10}$$

where $\delta\boldsymbol{M}_j$ and $\delta\boldsymbol{K}_j$ $\left(j = 1, ..., N_B\right)$ is the mass and stiffness mistuning matrices of j-th blade. Their 1st and 2nd derivatives with respect to the mistuning parameters b_j and b_k take the form:

$$\delta\boldsymbol{M}' = diag\left(\boldsymbol{0}, \boldsymbol{0}, ..., \delta\boldsymbol{M}'_j, ..., \boldsymbol{0}\right) \;\; ; \;\; \delta\boldsymbol{K}' = diag\left(\boldsymbol{0}, \boldsymbol{0}, ..., \delta\boldsymbol{K}'_j, ..., \boldsymbol{0}\right) \tag{11}$$

$$\delta\dot{\boldsymbol{M}}' = diag\left(\boldsymbol{0}, \boldsymbol{0}, ..., \delta_{jk}\delta\dot{\boldsymbol{M}}'_j, ..., \boldsymbol{0}\right); \;\; \delta\dot{\boldsymbol{K}}' = diag\left(\boldsymbol{0}, \boldsymbol{0}, ..., \delta_{jk}\delta\dot{\boldsymbol{K}}'_j, ..., \boldsymbol{0}\right) \tag{12}$$

where δ_{jk} is the Kronecker symbol, i.e. $\delta_{jk} = 1$ for $j = k$ and $\delta_{jk} = 0$ for $j \neq k$. Taking into account the expression for the FRF matrix in Eq.(4) and using these mass and stiffness matrix sensitivities we can calculate the first and second order displacement sensitivities in the form similar to the calculation of mistuned complex amplitudes (see Eq.(5)):

$$\frac{\partial\boldsymbol{x}}{\partial b_j} = \sum_{r=1}^{m}\frac{d_r^{(j)}\boldsymbol{\phi}_r}{(1+i\eta_r)\omega_r^2 - \omega^2}; \quad \frac{\partial^2\boldsymbol{x}}{\partial b_j\partial b_k} = \sum_{r=1}^{m}\frac{d_r^{(jk)}\boldsymbol{\phi}_r}{(1+i\eta_r)\omega_r^2 - \omega^2} \tag{13}$$

where $d_r^{(j)}$ and $d_r^{(jk)}$ are the coefficients of the expansion of the 1st and 2nd order sensitivity coefficients over the mode shapes of the mistuned bladed disk. The vectors comprising these coefficients for all mode shapes are obtained by multiplying the expressions in parentheses on the right hand of Eqs. (8) and (9) by mode shape matrix $\boldsymbol{\Phi}^T$ and taking into account the special form of mistuning matrix derivatives given by Eqs.(11) and (12):

$$\boldsymbol{d}^{(j)} = -\boldsymbol{\Phi}^T\left(\delta\boldsymbol{K}' - \omega^2\delta\boldsymbol{M}'\right)\boldsymbol{x} = -\boldsymbol{\Phi}_j^T\left(\delta\boldsymbol{K}_j' - \omega^2\delta\boldsymbol{M}_j'\right)\boldsymbol{x}_j = -\boldsymbol{D}_j'\boldsymbol{x}_j \tag{14}$$

$$\boldsymbol{d}^{(jk)} = -\boldsymbol{\Phi}^T\left[\left(\delta\dot{\boldsymbol{K}}' - \omega^2\delta\dot{\boldsymbol{M}}'\right)\boldsymbol{x} + \left(\delta\boldsymbol{K}' - \omega^2\delta\boldsymbol{M}'\right)\dot{\boldsymbol{x}} + \left(\delta\dot{\boldsymbol{K}} - \omega^2\delta\dot{\boldsymbol{M}}\right)\boldsymbol{x}'\right] = -\left(\delta_{jk}\boldsymbol{D}_j''\boldsymbol{x}_j + \boldsymbol{D}_j'\dot{\boldsymbol{x}}_j + \dot{\boldsymbol{D}}_k\boldsymbol{x}_k'\right) \tag{15}$$

where $\dot{\boldsymbol{D}}_k = \boldsymbol{\Phi}_k^T\left(\delta\dot{\boldsymbol{K}}_k - \omega^2\delta\dot{\boldsymbol{M}}_k\right)$; $\boldsymbol{D}_j'' = \boldsymbol{\Phi}_j^T\left(\delta\boldsymbol{K}_j'' - \omega^2\delta\boldsymbol{M}_j''\right)$ and subscripts j or k in $\boldsymbol{\Phi}_j^T$ and $\boldsymbol{\Phi}_k^T$ indicate that the mode shape matrices are selected for DOFs belonging only to j-th or k-th sector of the bladed disk. It should be noted that the matrices $\boldsymbol{D}_j'$ and $\dot{\boldsymbol{D}}_k$ used for the calculation of the second order forced response sensitivities are already obtained when coefficients for 1st order sensitivities are calculated in Eq.(14) and the additional computational efforts for the evaluation of 2nd order sensitivities are moderate. Moreover, the matrix products $\boldsymbol{\Phi}_j^T\delta\dot{\boldsymbol{K}}_j$ and $\boldsymbol{\Phi}_j^T\delta\dot{\boldsymbol{M}}_j$ can be calculated only once, before the calculation of sensitivities for the whole frequency range, which also reduces the computational expense.

2.3 Sensitivity for complex nodal amplitudes: a case of blade frequency mistuning

In the section above the formulation for the sensitivity analysis is proposed for a general case: when the mistuning matrices $\delta\boldsymbol{K}$ and $\delta\boldsymbol{M}$ can result from any mistuning nature and causes. In this paper all numerical results are obtained for a case when the blade frequency mistuning is analysed, and this particular case of mistuning parameterization allows further simplification of the sensitivity analysis. For this case the blade mistuning parameter is the relative difference between the mistuned and tuned blade frequencies: $b_j = \left(f_j^m - f_0^m\right)/f_0^m$, where f_j^m and f_0^m are mistuned and tuned single blade natural frequencies. The blade mode number, m, used for mistuning description can be chosen depending on the availability of the experimental data and the frequency range in which the mistuning forced response is analysed. For the blade frequency mistuning modelling a set of lumped masses is applied over nodes of a blade finite element model and the sector reference mistuning mass matrix, $\delta\boldsymbol{M}^S$, which is a diagonal matrix with values of the lumped masses, δm_j, located at the main diagonal of this matrix:

$$\delta\boldsymbol{M}^S = diag(0,...,0,\delta m_1,0,...,0,\delta m_2,0,...,0,\delta m_N,0...,0) \tag{16}$$

The additional masses are applied not to all nodes of the FE model but to a relatively small set of nodes: usually around $10^2 \ldots 10^4$ nodes on the blade surface which is much smaller than the total number of DOFs in the FE model, hence, the most of main diagonal entries are zeros. The distribution of the lumped masses are kept the same for all mistuned blades (as it is done in Refs. [21] and [22]) and in order to obtain j-th blade with the required mistuning the reference mistuning matrix is multiplied by a coefficient $\mu_j = \mu\left(b_j\right)$ which is dependent on the required mistuning level:

$$\delta\boldsymbol{M}_j = \mu\left(b_j\right)\delta\boldsymbol{M}^{\boldsymbol{S}} = \mu_j\delta\boldsymbol{M}^{\boldsymbol{S}} \tag{17}$$

The dependency of this coefficient $\mu\left(b_j\right)$ on the mistuning level is obtained as a result of performing of numerical analysis of resonance frequencies for a single blade (see Ref.[22]). The mass mistuning matrix of a whole bladed disk takes the form:

$$\delta\boldsymbol{M} = diag(\mu_1\delta\boldsymbol{M}^{\boldsymbol{S}},\mu_2\delta\boldsymbol{M}^{\boldsymbol{S}},...,\mu_{N_B}\delta\boldsymbol{M}^{\boldsymbol{S}}) \tag{18}$$

Taking first and second derivatives of Eq.(18) with respect to blade frequency mistuning parameters b_j and b_k we obtain:

$$\frac{\partial\delta\boldsymbol{M}}{\partial b_j} = diag\left(\boldsymbol{0},\boldsymbol{0},...,\frac{\partial\mu\left(b_j\right)}{\partial b}\delta\boldsymbol{M}^S,...,\boldsymbol{0}\right) \tag{19}$$

$$\frac{\partial}{\partial b_k}\left(\frac{\partial\delta\boldsymbol{M}}{\partial b_j}\right) = diag\left(\boldsymbol{0},\boldsymbol{0},...,\delta_{jk}\frac{\partial^2\mu\left(b_j\right)}{\partial b^2}\delta\boldsymbol{M}^S,...,\boldsymbol{0}\right) \tag{20}$$

Taking into account that for the accepted here approach for the blade frequency mistuning modelling $\delta\boldsymbol{K} = \boldsymbol{0}$ the coefficients for the modal expansion for 1st and 2nd order sensitivity coefficients (see Eq.(13)) take the following form:

$$\boldsymbol{d}^{(j)} = \boldsymbol{\Phi}^T \left(\delta \boldsymbol{M}' \boldsymbol{x}\right) = \omega^2 \frac{\partial \mu\left(b_j\right)}{\partial b} \left(\boldsymbol{\Phi}_j^T \delta \boldsymbol{M}^S \boldsymbol{x}_j\right) \tag{21}$$

$$\boldsymbol{d}^{(jk)} = \omega^2 \boldsymbol{\Phi}^T \left(\delta \dot{\boldsymbol{M}}' \boldsymbol{x} + \delta \boldsymbol{M}' \dot{\boldsymbol{x}} + \delta \dot{\boldsymbol{M}} \boldsymbol{x}'\right) = \omega^2 \left(\delta_{jk} \frac{\partial^2 \mu\left(b_j\right)}{\partial b^2} \boldsymbol{\Phi}_j^T \delta \boldsymbol{M}^S \boldsymbol{x}_j + \frac{\partial \mu\left(b_j\right)}{\partial b} \boldsymbol{\Phi}_j^T \delta \boldsymbol{M}^S \dot{\boldsymbol{x}}_j + \frac{\partial \mu\left(b_k\right)}{\partial b} \boldsymbol{\Phi}_k^T \delta \boldsymbol{M}^S \boldsymbol{x}_k' \right) \tag{22}$$

It should be noted that owing to the fact that matrix $\delta \boldsymbol{M}^S$ is diagonal with sparsely-spaced non-zero entries and the matrix products $\boldsymbol{\Phi}_j^T \delta \boldsymbol{M}^S$ are calculated once and then used in all expressions in Eqs.(21) and (22) the forced response sensitivities can be calculated sufficiently fast.

2.4 Sensitivity for the maximum displacement

For the first order sensitivity of the maximum displacement with respect to blade frequency mistuning parameter, b_j, the dependency on three coordinate components of complex amplitudes is taken into account:

$$\frac{\partial a}{\partial b_j} = \sum_{\alpha=x,y,z} \frac{\partial a}{\partial u_\alpha^{\mathrm{Re}}} \frac{\partial u_\alpha^{\mathrm{Re}}}{\partial b_j} + \frac{\partial a}{\partial u_\alpha^{\mathrm{Im}}} \frac{\partial u_\alpha^{\mathrm{Im}}}{\partial b_j} = \mathrm{Re}\left(\frac{\partial \boldsymbol{u}^H}{\partial b_j} \frac{\partial a}{\partial \boldsymbol{u}} \right) \tag{23}$$

where ^{H} is a Hermitian conjugate; the sensitivity coefficients of the complex amplitudes, $\partial \boldsymbol{u} / \partial b_j$, can be obtained from Eq.(13). The three components of the complex vector $\partial a / \partial \boldsymbol{u} = \partial a / \partial \boldsymbol{u}^{\mathrm{Re}} + i \partial a / \partial \boldsymbol{u}^{\mathrm{Im}}$ are obtained by differentiation of Eq.(7) with respect to complex amplitudes, which gives the following expression:

$$\frac{\partial a}{\partial \boldsymbol{u}} = \frac{1}{2a} \left(\boldsymbol{u} + \frac{c_1}{c_2} \overline{\boldsymbol{u}} \right) \tag{24}$$

where $c_1 = \boldsymbol{u}^T \boldsymbol{u}$; $c_2 = \left| \boldsymbol{u}^T \boldsymbol{u} \right|$, or in coordinate form:

$$\frac{\partial a}{\partial u_\alpha^{\mathrm{Re}}} + i \frac{\partial a}{\partial u_\alpha^{\mathrm{Im}}} = \frac{1}{2a} \left(u_\alpha + \frac{c_1}{c_2} \overline{u}_\alpha \right); \quad \alpha = x, y, z \tag{25}$$

To write the expressions for 2nd order sensitivities in a compact form, an auxiliary vector is defined as: $\boldsymbol{w} = \left\{ u_x^{\mathrm{Re}}, u_x^{\mathrm{Im}}, u_y^{\mathrm{Re}}, u_y^{\mathrm{Im}}, u_z^{\mathrm{Re}}, u_z^{\mathrm{Im}} \right\}^T$. Furthermore, based on this vector, Eq.(23) can be rewritten as:

$$\frac{\partial a}{\partial b_j} = \sum_{\alpha=1}^{6} \frac{\partial a}{\partial w_\alpha} \frac{\partial w_\alpha}{\partial b_j} = \frac{\partial a}{\partial \boldsymbol{w}} \frac{\partial \boldsymbol{w}}{\partial b_j} \tag{26}$$

In order to obtain the 2nd order sensitivity coefficients of maximum displacement with respect to blade frequency mistuning, Eq.(26) is differentiated with respect to b_k, which gives:

$$\frac{\partial}{\partial b_k} \left(\frac{\partial a}{\partial b_j} \right) = \frac{\partial}{\partial b_k} \left(\frac{\partial a}{\partial \boldsymbol{w}} \frac{\partial \boldsymbol{w}}{\partial b_j} \right) = \left(\frac{\partial \boldsymbol{w}}{\partial b_k} \right)^T \boldsymbol{H} \frac{\partial \boldsymbol{w}}{\partial b_j} + \left(\frac{\partial a}{\partial \boldsymbol{w}} \right)^T \frac{\partial^2 \boldsymbol{w}}{\partial b_j \partial b_k} \tag{27}$$

where the second order sensitivity coefficients of complex amplitudes, $\partial^2 \boldsymbol{w} / \partial b_j \partial b_k$, are obtained from Eq.(13) and matrix $\boldsymbol{H} = \left[\frac{\partial^2 a}{\partial w_\alpha \partial w_\beta} \right], (\alpha, \beta = 1,2,...,6)$ is obtained by differentiating Eq.(25) with respect to components of vector $\boldsymbol{w}$:

$$\frac{\partial}{\partial u_\beta^{\mathrm{Re}}} \left(\frac{\partial a}{\partial u_\alpha^{\mathrm{Re}}} + i \frac{\partial a}{\partial u_\alpha^{\mathrm{Im}}} \right) = \frac{-1}{a} \frac{\partial a}{\partial u_\beta^{\mathrm{Re}}} \left(\frac{\partial a}{\partial u_\alpha^{\mathrm{Re}}} + i \frac{\partial a}{\partial u_\alpha^{\mathrm{Im}}} \right) + \frac{1}{a} \left[\left[2\delta_{\alpha\beta} + \frac{u_\beta \overline{u}_\alpha}{c_2} + \frac{c_1}{c_2} \left(2\delta_{\alpha\beta} - \frac{\mathrm{Re}\left(\overline{u}_\beta c_1 \right)}{c_2^2} \overline{u}_\alpha \right) \right] \right] \tag{28}$$

$$\frac{\partial}{\partial u_\beta^{\mathrm{Im}}} \left(\frac{\partial a}{\partial u_\alpha^{\mathrm{Re}}} + i \frac{\partial a}{\partial u_\alpha^{\mathrm{Im}}} \right) = \frac{-1}{a} \frac{\partial a}{\partial u_\beta^{\mathrm{Im}}} \left(\frac{\partial a}{\partial u_\alpha^{\mathrm{Re}}} + i \frac{\partial a}{\partial u_\alpha^{\mathrm{Im}}} \right) + \frac{1}{2a} \left[i\delta_{\alpha\beta} + i \frac{2u_\beta \overline{u}_\alpha}{c_2} - \frac{c_1}{c_2} \left(i\delta_{\alpha\beta} + 2 \frac{\mathrm{Im}\left(c_1 \overline{u}_\beta \right)}{c_2^2} \overline{u}_\alpha \right) \right] \tag{29}$$

where

$$\delta_{\alpha\beta} = \begin{cases} 1, & \text{for} \quad \alpha = \beta \\ 0, & \text{for} \quad \alpha \neq \beta \end{cases} \quad ;\alpha,\beta = x,y,z \tag{30}$$

3. OPTIMIZATION ALGORITHMS FOR RESPONSE PREDICTION OF MISTUNED BLADED DISKS

For gas-turbine engine industry applications it is important to know what are the best and worst mistuning patterns – the patterns which provide the minimum and maximum forced response levels respectively for a mistuned bladed disk of a chosen design. This knowledge allow assessing possible variations of the response levels during engine service and within a fleet of manufactured engines. The problem of the continuous optimization for a mistuned bladed disk is formulated in the form:

$$\begin{array}{ll} \text{for worst mistuning} & \text{for best mistuning} \\ a(\boldsymbol{b}) \rightarrow \max & a(\boldsymbol{b}) \rightarrow \min \end{array} \tag{31}$$

with the constraints

$$\boldsymbol{b}^- \leq \boldsymbol{b} \leq \boldsymbol{b}^+ \tag{32}$$

where $\boldsymbol{b}^-$ and $\boldsymbol{b}^+$ are vectors containing low and high limits of mistuning parameter variation respectively.
Moreover, when a specific set of mistuned blades is provided for a bladed disk it is useful to have the information how to assemble them in a bladed disk in the way which provides the minimum response levels and also to avoid the blade arrangement in a bladed disk which provides the maximum response levels. To obtain the best and worst blade arrangements in a bladed disk a combinatorial optimization problems are formulated and solved. The objective functions for this optimization problem have the same form as used for the continuous optimization (see Eq.(31)), but the constraints reflect the fact that the set of blade mistuning is fixed and only their arrangement in the bladed disk can be chnaged, i.e. blade mistuning permutation can be only performed in the mistuning parameter vector. This condition can be written in the following form:

$$\boldsymbol{b} \subseteq \boldsymbol{b}_* \tag{33}$$

where $\boldsymbol{b}_*$ is the set of mistuning parameters provided for the set of blades intended to be assembled in a disk.
The efficiency of different optimization algorithms are explored for solution of the mistuned bladed disk forced response optimization problems. In this section the algorithms studied are briefly described for these two types of the optimization problems.

3.1 Searching the worst and best mistuning patterns based on gradient information

The developed method for sensitivity coefficient calculation described in the previous section is used to obtain the gradient information of the maximum forced response displacements of mistuned bladed disks. In all 4 optimization algorithms explored here the 1st order sensitivity coefficients are used. In addition to this the trust-region algorithm uses the 2nd order sensitivity coefficients. The search of the best and worst mistuning patterns is formulated here as a continuous optimization problem with the bound constraints imposed by acceptable blade mistuning variations. The following algorithms are applied for the optimization problem.

Algorithm 1. Interior-point algorithms (see Refs.[25] - [27]) have a reputation to be efficient for the optimization problems with large number of design variables and constraints which is the advantage for the mistuning optimization when there are usually many blade mistuning parameters. The algorithms are based on the Newton's method, which is applied to the optimization objective function and the barrier functions keeping the solution point during the optimization search within the domain described by the constraints.

Algorithm 2. Trust-region algorithms (see Refs. [28] and [29]) generate the iterative solution steps with the help of a quadratic approximations of the objective function based on the Hessian of the objective function. The region where the quadratic approximation have acceptable accuracy is deemed the trusted region and the iteration step is chosen basing on this approximation: both the direction of the step and the step size are selected. The size of the trusted region is varied during the optimization iterations depending on the success of the iteration steps and the size of the trust region is critical to the effectiveness of the optimization search. In practical algorithms, the region is chosen according to the performance of the algorithm during previous iterations. A failed optimization step indicate that the trust region is too large and the size of the region should be reduced.

Algorithm 3. Sequential quadratic programming (SQP) algorithm (see Refs.[30] and [31]) is applied for nonlinear constrained optimization problems, it generates optimization steps by solving quadratic sub-problems for each iteration.

SQP is assumed especially effective when the constraints are linear function or bounds as is the case of the blade mistuning constraints.

Algorithm 4. Active-set algorithms (Refs. [32] and [33]) are usually effective for problems with small and medium numbers of optimization parameters and based on the selecting the 'active' inequality constraints (i.e. the constraints which restrict the optimization iteration step) and transforming these constraints into equality constraints at each iteration.

3.2 Combinatorial optimization for mistuned blades

Searching for the best and worst combinations of a specific set of mistuned blades is a combinatorial optimization problem, and the genetic algorithm is employed to perform this search [20]. The algorithm below is formulated for the case of search for the best mistuning arrangement. A search for the worst mistuning arrangement can be performed using the same algorithm but alternating signs upon the mistuned amplitudes in the formulas for probabilities used in the selection and crossover operations. The procedure for combinatorial optimization based on the genetic algorithm contains the following major steps.

Step.1. Initialization. A population, $\boldsymbol{B}_0$, of mistuning vectors, $\boldsymbol{b}_j$, is randomly generated from the given set of values of mistuned blades, $\boldsymbol{b}_*$, i.e.

$$\boldsymbol{B}_0 = \{\boldsymbol{b}_1, \boldsymbol{b}_2, \cdots, \boldsymbol{b}_n\}; \quad \boldsymbol{b}_j \subseteq \boldsymbol{b}_* \tag{34}$$

where n is the total number of mistuning vectors generated for the population used for the optimization. Vectors $\boldsymbol{b}_j$ are generated by random permutation of the given set of blades, $\boldsymbol{b}_*$. This population is adopted as initial generation $\boldsymbol{B}_k$ with the starting generation number: $k = 0$.

Step.2. Selection. The maximum nodal forced response displacement, $a(\boldsymbol{b}_j)$, of the bladed disk is calculated for each $\boldsymbol{b}_j$ for the generation $\boldsymbol{B}_k$. Then, the probability of keeping the *j*-th mistuning pattern, $\boldsymbol{b}_j$, for the next generation is determined as:

$$p_j = \frac{a^{\max} - a(\boldsymbol{b}_j)}{n\left(a^{\max} - a^{\text{mean}}\right)}; j \in [1, n] \tag{35}$$

where

$$a^{\max} = \max_{j \in [1,n]}\left(a(\boldsymbol{b}_j)\right); \quad a^{\text{mean}} = \frac{1}{n}\sum_{j=1}^{n} a(\boldsymbol{b}_j) \tag{36}$$

Based on the calculated probability for each blade arrangement in the bladed disk, and the mistuning arrangements providing lower response levels this probability is higher.

Step.3. Crossover. All the mistuning arrangement vectors are combined into pairs and the values of the counterparts are exchanged depending on the crossover probability, p_c, which can be chosen, for example, 0.8. It should be noted that the special control of exchanged patterns is performed to satisfy the requirement that all values of obtaining as result of the crossover mistuning vectors are taken from $\boldsymbol{b}_*$ without repetitions. The result of the crossover provides the next generation, $\boldsymbol{B}_{k+1}$.

Step.4. Mutation: For each mistuning vector from generation $\boldsymbol{B}_{k+1}$ the binary random generator is run to obtain value 1 (there is mutation) or 0 (no mutation) with the prescribed mutation probability, p_m. The mutation of the mistuning vector is performed for value 1. The mutation operation consists in random choice of the number of the mistuning vector component. The value of this component is substituted by a value from a given set of mistuned blades, $\boldsymbol{b}_*$, which is chosen randomly too. The check is performed also to exclude repetition of the values for different components of the mistuning vector.

Step.5. Termination check. The optimization process is terminated when the limit number of generations is achieved, otherwise the optimization process goes to Step 2.

4. NUMERICAL RESULTS

The high-fidelity finite element model of a turbine bladed disk shown in Fig. 1 is used for the analysis of the sensitivities and for the solution of the formulated optimization problems. The bladed disk comprises 86 shrouded blades and the total number of degrees of freedom (DOFs) is about 7.35 millions. Based on the cyclic symmetry properties of tuned bladed

disks, a single sector of this bladed disk is used to obtain the natural frequencies and corresponding mode shapes of the tuned bladed disk for all the nodal diameters (for the considered model the number of nodal diameters varies from 0 to 43). The dependency of natural frequencies of the tuned bladed disk on nodal diameters is shown in Fig. 2.

The engine-order (EO) excitations by 4 (when the disk coupling is significant) and 22 engine orders (when the stiffness of the disk is high and the disk coupling effect is low) are considered. Moreover the excitation frequency ranges are chosen to excite vibration in low and high frequency ranges. The excitation frequency ranges and EOs are marked in Fig. 2 as '4EO-low' (the excitation frequency range is 1100~1400Hz), '4EO-high' (17500~19500Hz), '22EO-low' (1200~1350Hz), and '22EO-high' (14000~15000Hz). The damping factor is assumed 0.003 in most calculations, for cases when other values are used it is specified in the text.

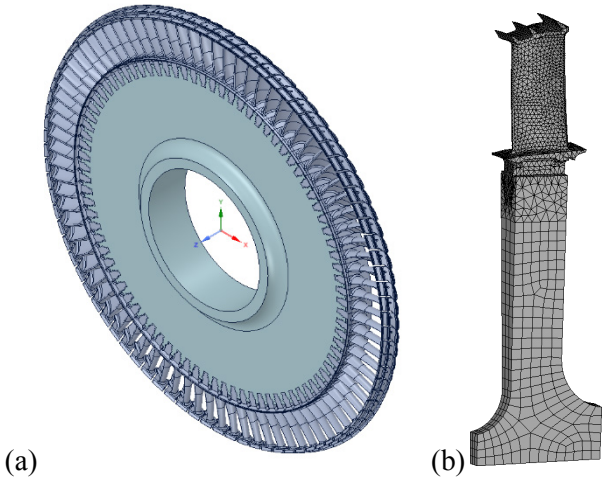

Fig. 1 Finite element model: (a) a bladed disk; (b) a sector

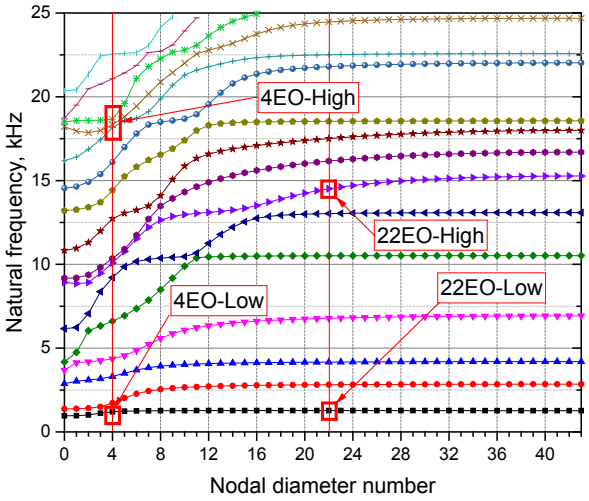

Fig. 2 Natural frequencies of the tuned assembly

4.1 Sensitivity coefficient analysis

In this section, the first and second order sensitivity coefficients of maximum forced response displacements with respect to frequency mistuning of blades are investigated. Firstly, four types of blade frequency mistuning patterns are explored for the calculation of the sensitivity coefficients: (i) a perfectly tuned bladed disk; (ii) an alternate mistuning pattern, i.e. each blade with +5% mistuning has neighbouring blades with mistuning -5%; (iii) a harmonic mistuning pattern, when the blade frequency distribution over blades is described by function (where is the blade number); (iv) a random mistuning pattern. All these mistuning patterns are shown in Fig. 3. First three of these mistuning patterns are often considered as candidates for the intentionally introduced mistuning and there is some interest to explore the sensitivities of the forced response for these patterns together with the random mistuning pattern. The frequency dependency of the normalized forced response levels for the whole bladed are plotted for these patterns in Fig. 4. The response normalization is performed by dividing the maximum mistuned response by the maximum tuned forced response calculated over the frequency range analysed. The

tuned bladed disk has one resonance peak in the frequency range analysed and the forced response of alternative mistuning pattern has two resonance peaks, since this pattern leads to the reduction of the cyclic symmetry order by factor of 2 and, therefore, to the occurrence of an additional resonance peak. The harmonic and random mistuning patterns provide a multitude of resonance peaks. The random mistuning pattern has higher maximum response level than the others.

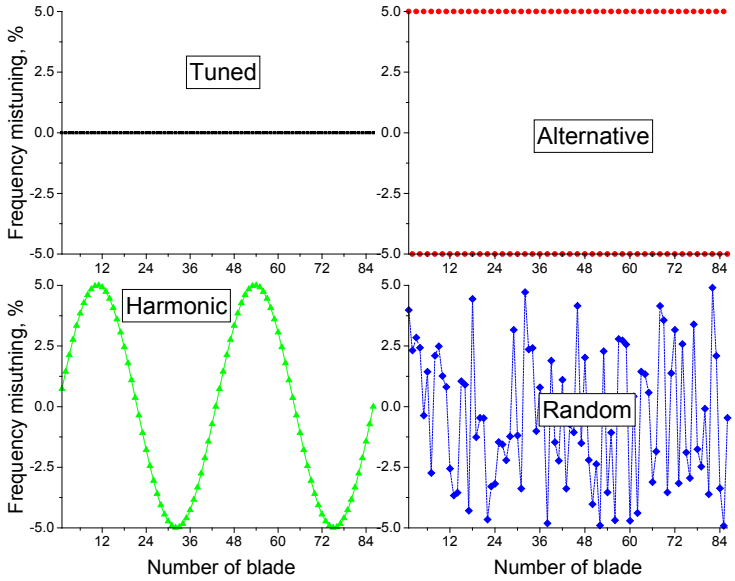

Fig. 3 Mistuning patterns studied in the sensitivity analysis

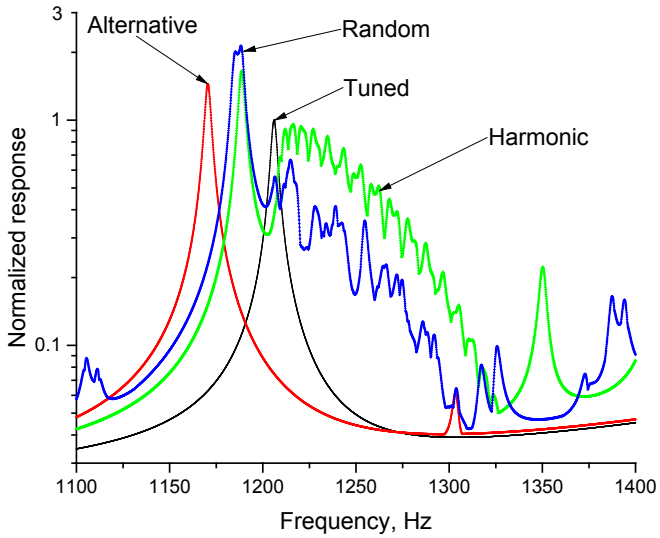

Fig. 4 Normalized response levels under 4EO-low excitation

The maximum forced responses levels determined separately for each of the blades are shown in Fig. 5. It is obvious that: (i) for the tuned bladed disk, all the blades have same maximum values; (ii) for the alternative mistuning pattern, the maximum forced response of each blade alternates to two response levels (since the bladed disk also can be considered as a tuned system, but the sector is consisted of two adjacent sectors of original system); (iii) for the harmonic mistuning pattern, the distribution of maximum responses of each blade are periodic and also close to harmonic; (iv) for the random mistuning pattern, the distribution of maximum response of blades is also random for the considered bladed disk.

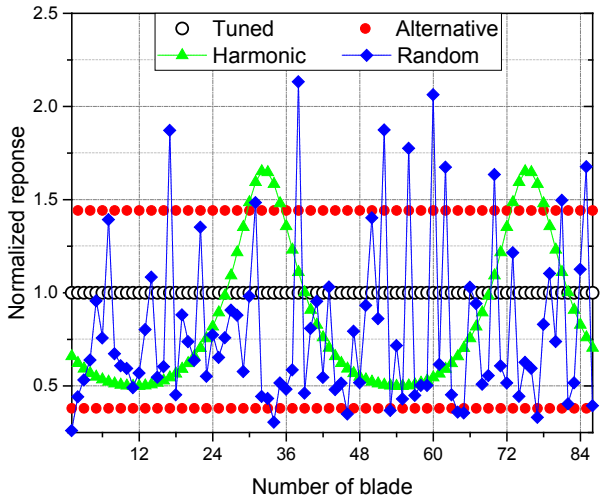

Fig. 5 Normalized response displacements of blades

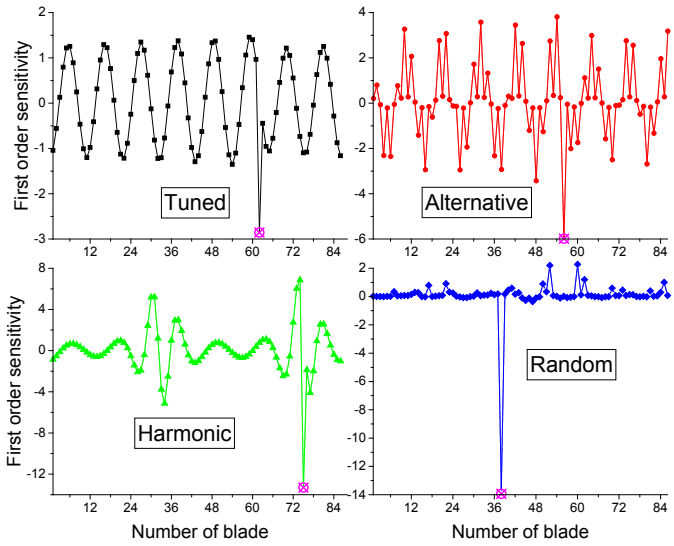

Fig. 6 1st order sensitivity coefficients for the bladed disk response wrt blade frequency mistuning

The first order sensitivity coefficients of the maximum bladed disk response are shown in Fig. 6. For the tuned assembly and for alternative and harmonic mistuning patterns, the sensitivity coefficients for the maximum blade responses are close to periodic the number of periods 8, which is the excitation EO number multiplied by 2. For the random mistuning pattern is random, the first order sensitivity coefficients do not have a distinct pattern and the coefficients corresponding to blade maximum responses low, except for one blade – which is the blade where the maximum level is achieved. It should be noted that for the blade where the maximum response is achieved there is an evident sharp change of the sensitivity coefficients. Such maximum is achieved here at blade 62 - for tuned bladed disk, 56 - for alternative mistuning, 75 - for harmonic mistuning, and 38 - for random mistuning.

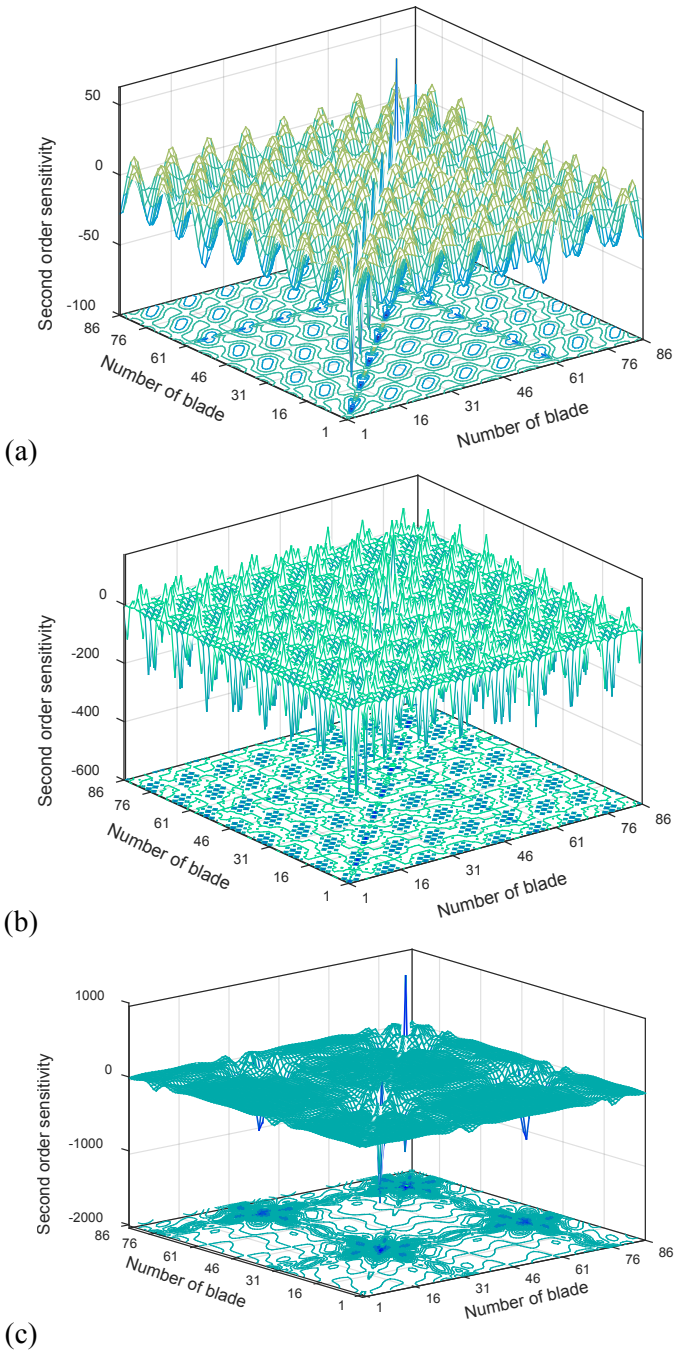

Fig. 7 Second order sensitivity coefficients wrt blade mistuning (4EO): a) tuned; b) alternative; c) harmonic mistuning

The matrix of second order sensitivity coefficients, $\left[\partial^2 a / \partial b_j \partial b_k\right]$, of maximum forced response displacement with respect to blade mistuning parameters provides also important information for analysis and optimization of the response characteristics. The examples of graphic representation of this matrix are shown in Fig. 7 for three representative cases: a tuned bladed disk, alternative and harmonic mistuning patterns shown in Fig. 3. The sensitivities are plotted for the excitation frequency corresponding to the maximum resonance peak forced response level. One can see that the mistuning of all blades have significant values of the sensitivity coefficients, although the terms belonging to the main diagonal of the 2nd order sensitivity matrix are dominant.

4.2 Optimization searching of best and worst mistuning patterns

In the search of the best and worst mistuning patterns the constraints on the mistuning variation are imposed: $-5\% \le \boldsymbol{b} \le 5\%$. Firstly, the efficiency of four optimization algorithms mentioned above has been explored for the search of the best and worst mistuning patterns of mistuned bladed disks. The initial mistuning patterns are randomly generated

and chosen the same for all optimization algorithms. The example of convergence of the optimization process with the number of iterations is demonstrated in Fig. 8 for cases of searching for the best and worst mistuning under 4EO-low excitation. Similar results were obtained for all specified in Fig. 2 frequency ranges and EOs. The comparison of the optimization search results obtained by different algorithms allows us to conclude that: the SQP algorithm was efficient for the search of worst mistuning, and the interior-point algorithm was efficient for the search of best mistuning. SQP and the interior-point algorithms are adopted for the search the worst and best mistuning patterns, respectively, in the studies reported below.

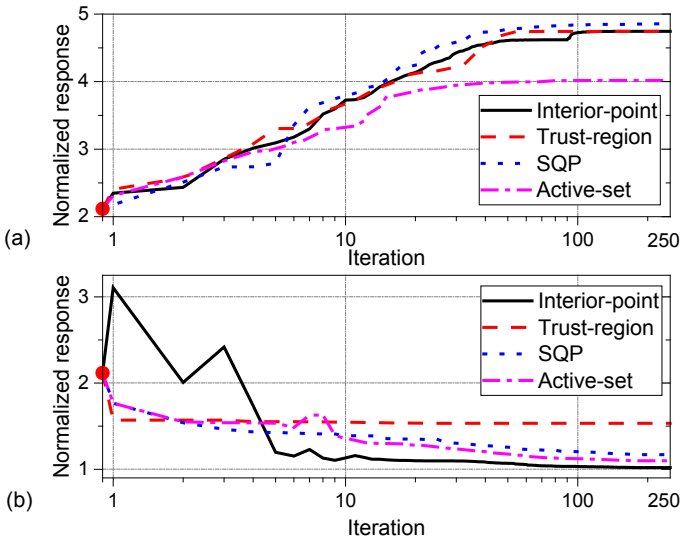

Fig. 8 Results of the optimization search obtained by different optimization algorithms: (a) worst mistuning; (b) best mistuning

The optimization problem formulated for the best and worst mistuning search is so called 'multi-modal' problem, i.e. it has not one but a multitude of the local extremums and, therefore, the optimization search can produce different optimization solutions when starting from different initial configurations. For the search of the global optimum, we may need to start the solution search from different initial mistuning patterns. The examples of optimization search dependency on the initial mistuning pattern is illustrated in Fig. 9 and Fig. 10 for cases of excitation by 4EO and 22 EO in the higher frequency ranges.

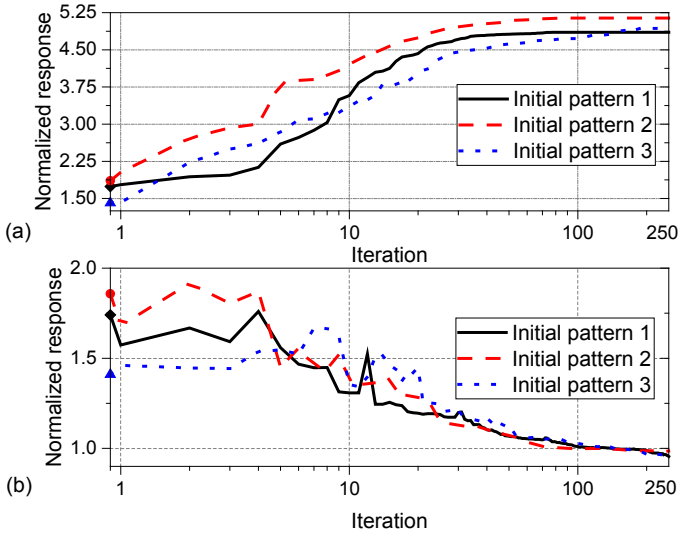

Fig. 9 Results of optimization searching for the case 4EO-high: (a) worst searching; (b) best searching

It is evident noticeable differences in the results of the optimization search for different starting points. Similar calculations have been made for the other excitation conditions (see Fig. 2). The maximum magnification factor found for the four cases considered are dependent on EOs and frequency ranges: 4.855 - for 4EO-low, 5.140 – for 4EO-high, 3.144 – for 22EO-low, and 5.145 – for 22EO-high. The Whitehead limit values for this bladed disk is: $0.5\left(1+\sqrt{N_B}\right)=5.137$, which is very close to

two of the considered cases corresponding to the high frequency ranges, but is too high for the low frequency ranges. In the search for the best mistuning patterns, it was found that the forced response of the mistuned bladed disk can reach a value which is little less than the tuned response.

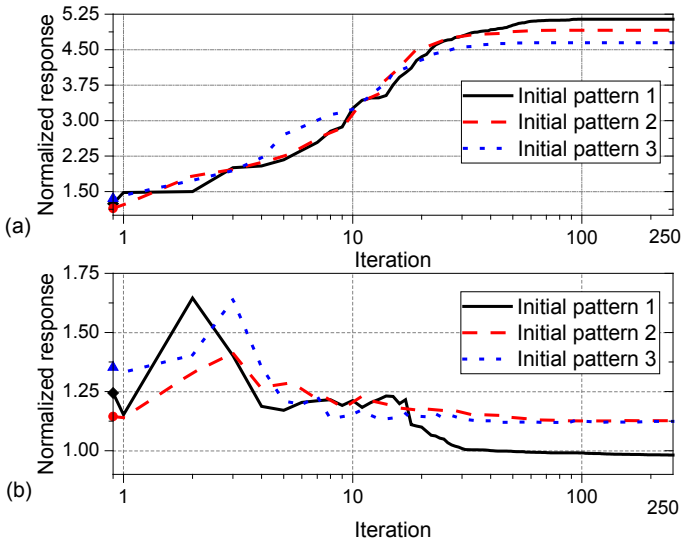

Fig. 10 Results of optimization searching for the case 22EO-high: (a) worst searching; (b) best searching

The initial mistuning patterns and the best and worst mistuning patterns found as a result of optimization are shown in Fig. 11 and Fig. 12 for cases 4EO-low and 4EO-high.

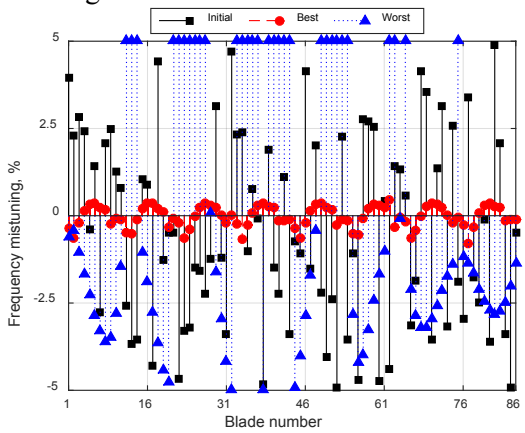

Fig. 11 The initial, best and worst mistuning patterns: 4EO-low

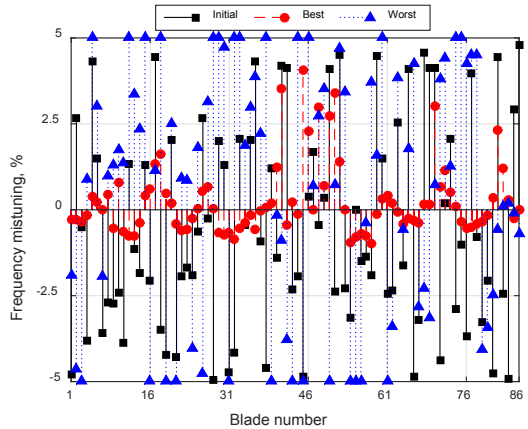

Fig. 12 The initial, best and worst mistuning patterns: 4EO-high

One can see that the worst mistuning patterns have large number of blades with the blade mistuning reached the low and upper boundary of acceptable mistuning, i.e. -5.0% and 5.0%. The best mistuning pattern for 4EO-low is close to the

harmonic distribution with the harmonic number equal to the EO number multiplied by factor of 2. For 4EO-high the best mistuning pattern differs significantly from the harmonic distribution although part of the mistuning pattern resembles this distribution distantly.

The distributions of maximum blade amplitudes are shown in Fig. 13 and Fig. 14 for the initial, best and worst mistuning patterns. One can see that for the case of the best mistuning the maximum blade amplitude distribution is periodic with 8 cycles over the bladed disk – for 4EO-low and close to periodic for 4EO-high. For the case of the worst mistuning the blade maximum amplitudes are localised at one of the blades of the bladed disk for low and high frequency ranges and the maximum blade amplitude level is higher than the rest blades by factor of 5.

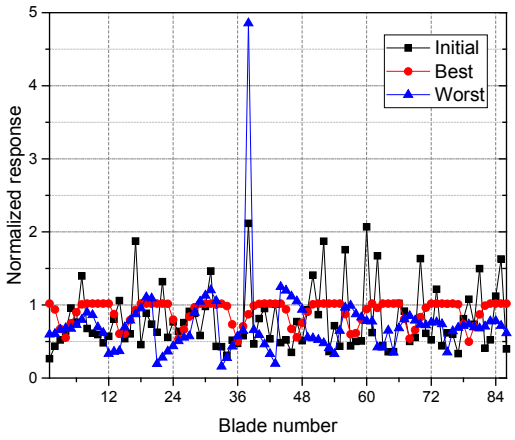

Fig. 13 The maximum blade amplitude distributions: 4EO-low

The frequency dependency of the envelopes of the bladed disk forced response are plotted for mistuned cases and for their tuned counterparts in Fig. 15 and Fig. 16. One can see that the forced response for the initial random mistuning pattern and for the worst mistuning patterns have many resonance peaks over a wide frequency range. The total number of resonance peaks observed here is much less than the total number of natural frequencies of the mistuned bladed disk (which has to be larger than the number of blades in one family of modes, i.e. 86) – this is due to effects of damping which merges some of the resonance peaks and, moreover, some other resonances dominate and make lower resonance peaks unnoticeable. The forced responses calculated for the found best mistuning patterns resemble generally the tuned response. They have almost the same maximum forced response levels, but the amplitudes in the out-of-resonance frequency ranges are significantly higher that the tuned response and minor resonance peaks appear due to blade mistuning.

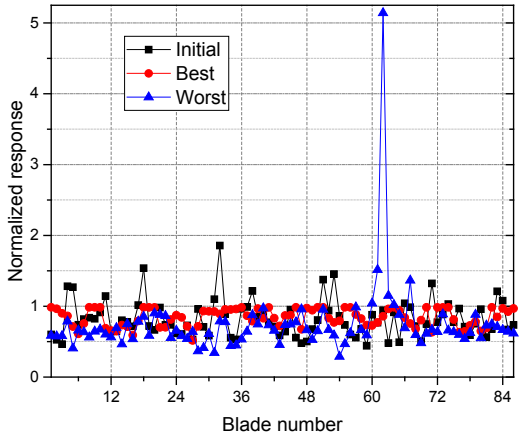

Fig. 14 The maximum blade amplitude distributions: 4EO-high

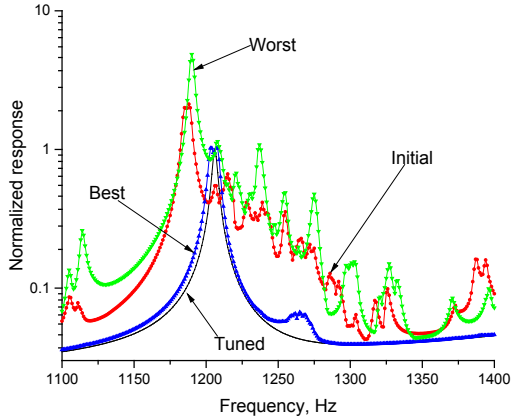

Fig. 15 Frequency dependency of the bladed disk maximum amplitude: 4EO-low

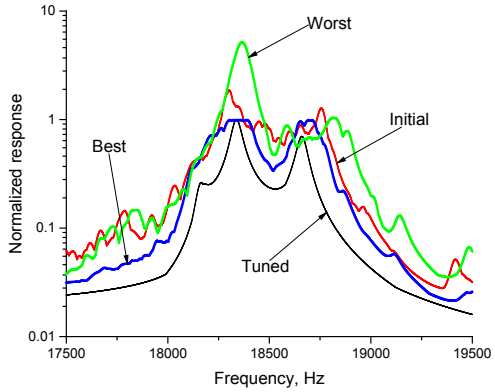

Fig. 16 Frequency dependency of the bladed disk maximum amplitude: 4EO-high

The 1st order sensitivities of the maximum bladed disk response calculated for the best and worst mistuning are plotted in Fig. 17. The theoretically the sensitivity coefficients should take zero values at the local minimum of the optimization problem without constraints. In the our cases the sensitivities are small for most blades but for some blades they are significant – which is due to effects of the bound constraints imposed on the mistuning variation and which are active at the found optimal point for the cases of worst mistuning.

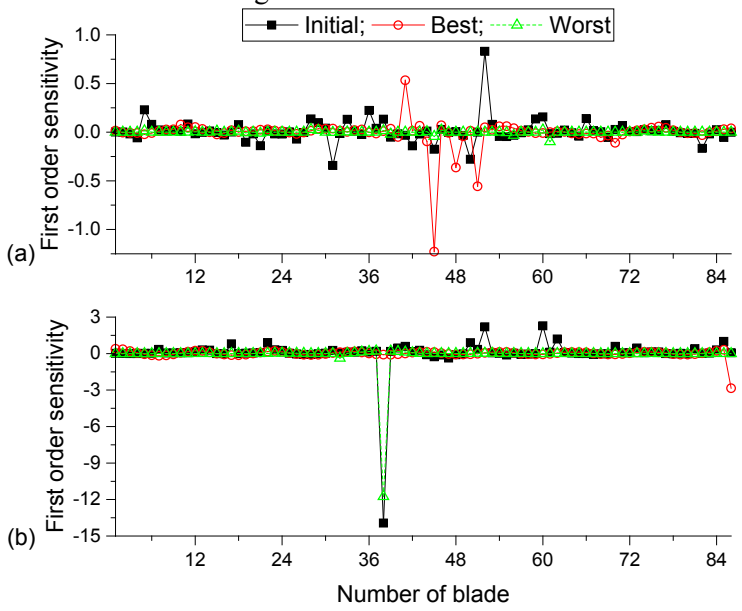

Fig. 17 Distributions of the first order sensitivities corresponding to the initial, best and worst mistuning patterns: (a) 4EO-high; (b) 4EO-low

1.1 Damping effects on best and worst mistuning

The effects of the damping levels on the optimization search and the amplification factors have been studied too. The examples of the convergence of the optimization search for different modal damping factors are shown in Fig. 18.

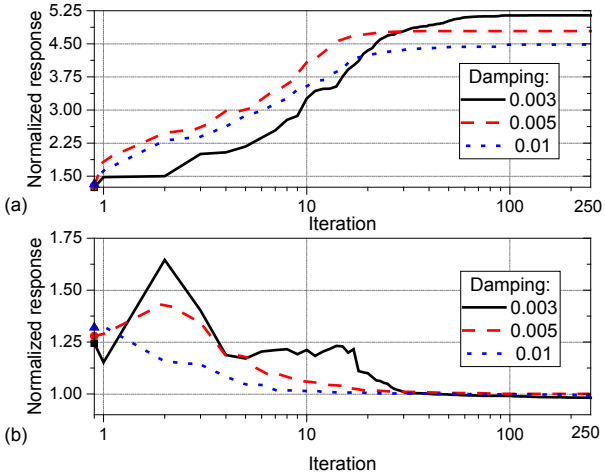

Fig. 18 Results of the optimization search obtained for different damping factors for 22EO-high: (a) worst mistuning; (b) best mistuning

It is interesting to note that the damping affects the worst amplification factor values but in the search for the best mistuning the amplification factors close to 1 are found for all considered damping levels. The dependency of the amplification factors for worst mistuning factors on the damping is shown in Fig. 19 for all excitation cases (see Fig. 2). One can see that for the considered cases the increase of damping decreases the worst amplification factor for all cases except the case of 4EO-low.

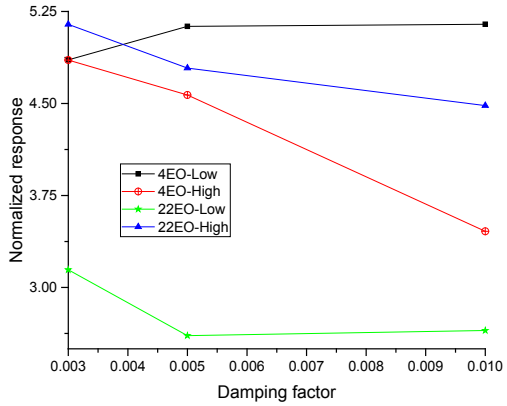

Fig. 19 Magnification factors obtained by different damping factors corresponding to worst searched for different cases

Fig. 20 presents the calculated mistuning patterns providing the highest response levels for the cases 4EO-low and 4EO-high excitation. The worst mistuning patterns differ for different mistuning ranges. For 4EO-low and the modal damping factor 0.003 (where the mistuning pattern is more regular) we can observe that in the worst mistuning pattern many blades reach the mistuning range constraints -5% or +5%, with the increase of the damping such a number of blade is reduced and the mistuning pattern has more localised shape.

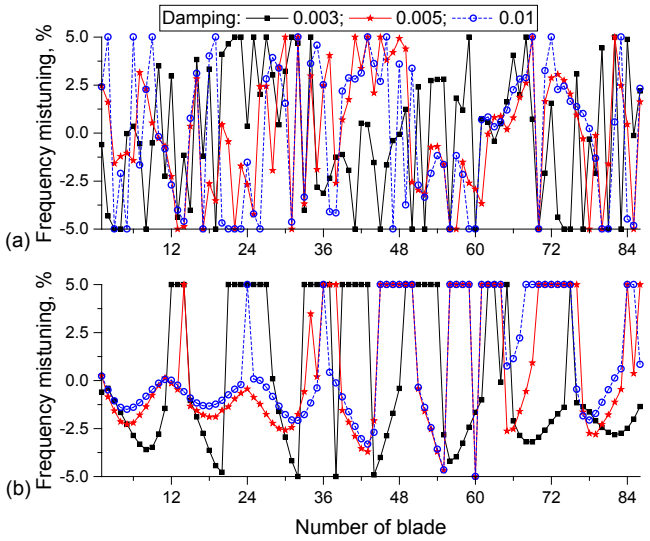

Fig. 20 Worst mistuning patterns for different damping factors: (a) 4EO-high; (b) 4EO-low

The examples of forced responses calculated for worst mistuning patterns with different damping levels are shown in Fig. 21 where they are compared with the tuned response. One can see that the number of the distinct resonance peaks is reduced with the damping increase but the amplification factor levels for bladed disks with higher damping become in out-of-resonance frequency ranges significantly higher than that for low damping cases. The distributions of maximum blade amplitudes are shown in Fig. 22. They are almost identical for damping factor values 0.005 and 0.010, but differ significantly from results obtained for damping factor 0.003

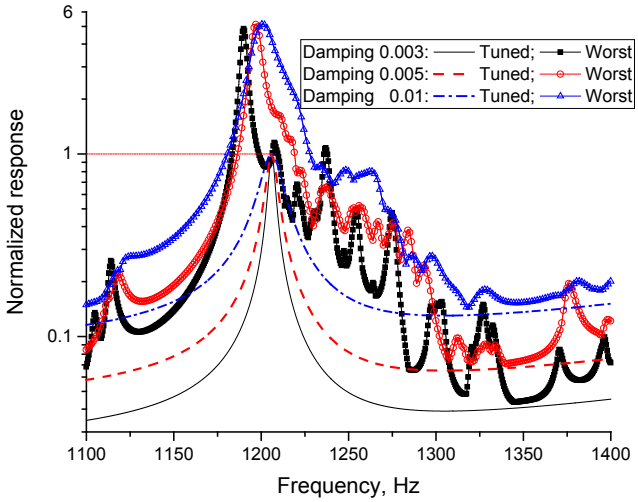

Fig. 21 Normalized responses for worst mistuning for different damping levels: 4EO-low

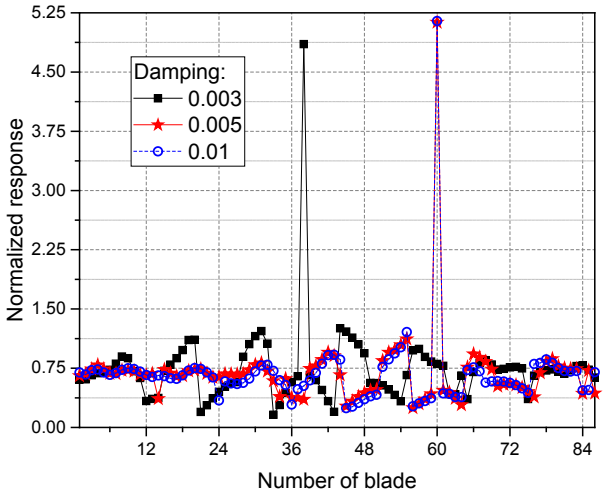

Fig. 22 The maximum blade amplitude distributions: 4EO-low for different damping levels

4.3 Combinatorial optimization of best and worst arrangements

In this section, the examples of studies of the best and worst mistuned blade arrangements in a bladed disk using the developed combinatorial optimization method are given. The number of mistuning bladed arrangements in one population was chosen to be 300 and the limiting number of generations is 250. The examples of the convergence of the optimization search for the worst arrangements of mistuned blades are shown in Fig. 23 for three different initial mistuning patterns.

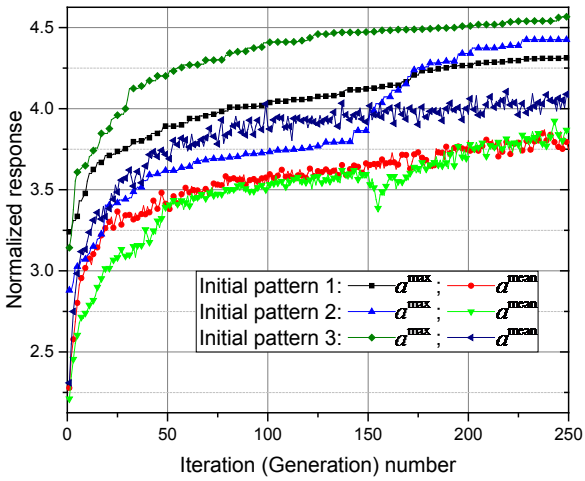

a)

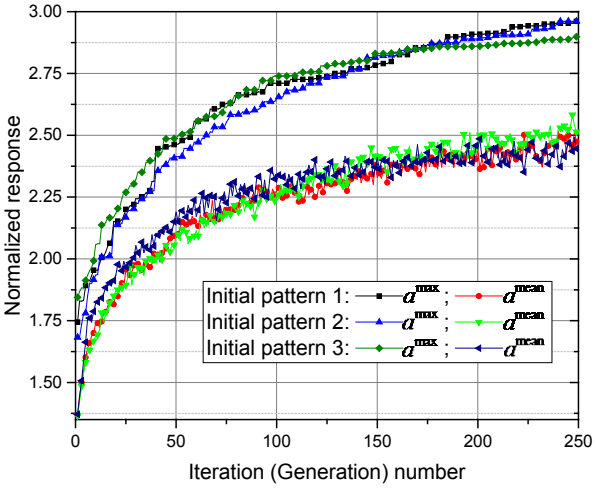

b)

Fig. 23 Combinatorial optimization convergence for the case of worst mistuning search (a) 4EO-low; (b) 22EO-low

Two characteristics are plotted here for each of 250 generations created during the optimization: the maximum amplification factor over all samples belonging to the generation, and the mean value calculated over all samples of the considered generation, . We can see that the blade arrangement affects the amplification factor very much. The highest amplification factors found by the blade rearrangements (when there is a restricted set of mistuned blades) are close to that found by the continuous optimization (when the blade mistuning can take any values from a given mistuning range) for considered here cases of 4EO-low and 22EO-low. Moreover, it is evident that the generation mean amplification factor for 22-low differs from the maximum value significantly more than for the case of 4EO-low excitation. Moreover, one can see that is practically not affected by the choice of the initial mistuning pattern for 22EO-low while such influence for 4EO-low is more significant.

The maximum blade amplitudes obtained for the initial, best and worst arranged mistuning patterns are shown in Fig. 24 and Fig. 25. The envelopes of the maximum amplitude bladed disk amplitudes are plotted in Fig. 26 and Fig. 27. Here the results corresponding to 4EO-low and 22EO-low are shown. Similar analysis has been performed for the other excitation conditions. For all analysed cases we observed that the worst blade arrangements produced highly localised blade amplitudes – similar to the case of the continuous optimization. The best mistuning patterns are far from any regular patterns – which contrasts to the continuous optimization case. The maximum forced response curves obtained in Fig. 26 and Fig. 27 for the best mistuning arrangements differ also significantly from the response obtained by the continuous optimization where the response was much closer to that of tuned assembly (see Fig. 15). The choice of blade rearrangement affects significantly not only the level of maximum response but also dominant resonance frequency values, while the frequency range width where the mistuned forced response is significant does not change with the blade rearrangements.

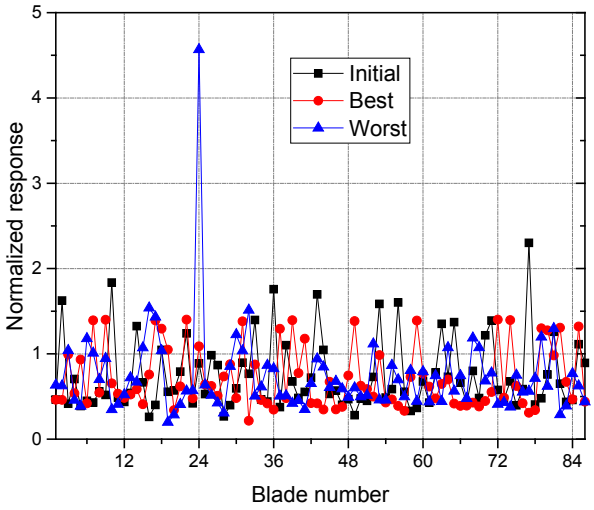

Fig. 24 The maximum blade amplitude distributions: 4EO-low

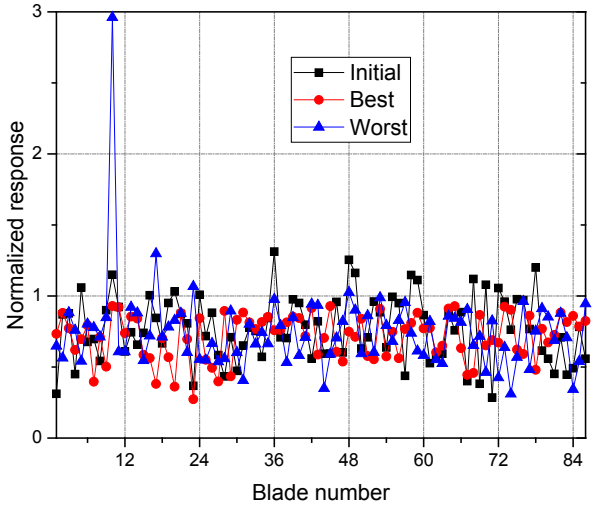

Fig. 25 The maximum blade amplitude distributions: 22EO-low

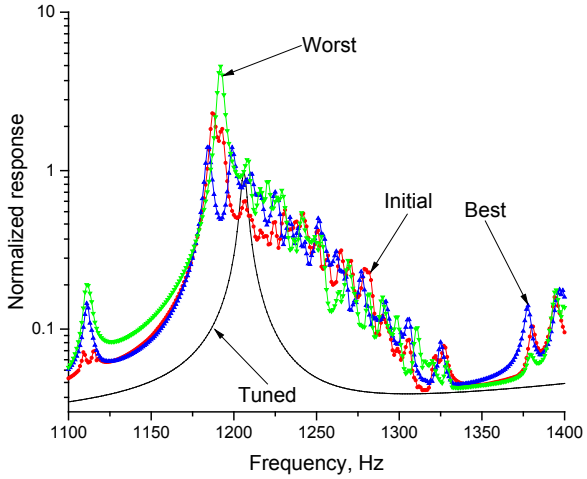

Fig. 26 Normalized bladed disk amplitudes for the initial, best and worst blade arrangements: 4EO-low

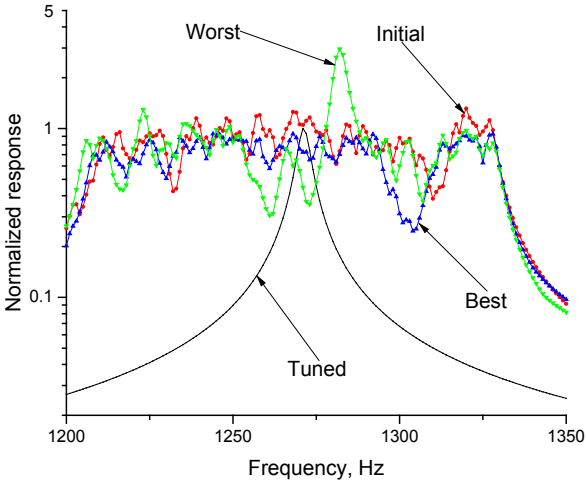

Fig. 27 Normalized bladed disk amplitudes for the initial, best and worst blade arrangements: 22EO-low

5. CONCLUSIONS

An effective method for the first and second order sensitivity coefficient calculations for the maximum forced response displacement of mistuned blade disks with respect to blade frequency mistuning parameters has been developed. The method allows the sensitivity analysis of large-scale realistic finite element models of bladed disks and all expressions are obtained in analytical form, which provides accurate and fast calculations.

The obtained sensitivities are used for the determination of the worst and best mistuning patterns and the corresponding lowest and highest forced response levels. The optimization problem is formulated for the search of such mistuning patterns and several gradient-based optimization methods have been explored and their efficiency have been assessed and compared. The problem of determining the best and worst mistuned blade arrangements – when a set of mistuned blades is given and only blade position can be changed – is considered. The problem is formulated as a combinatorial optimization problem and a variant of an optimization algorithm based on the genetic optimization methodology is developed.

The capabilities of the developed methods are demonstrated on the analysis of an industrial bladed disk finite element model vibrating in low and high frequency ranges. The 1st and 2nd order sensitivities of the maximum bladed disk forced response with respect to blade mistuning have been studied for intentional and random mistuning patterns.

The worst and best mistuning patterns and response levels have been calculated for this bladed disk for both types of the optimization problems: (i) continuous gradient-based optimization and (ii) combinatorial optimization of the blade

arrangement. The dependency of the worst and best mistuning patterns and the amplification factors on the damping levels has been analysed. The possibility to attain the Whitehead limit for the amplification factor by the optimization search for some of the excitation conditions is shown for both types of the optimization search. The possibilities for the alteration of the forced response amplitudes and the frequency range width corresponding to high response levels have been studied.

ACKNOWLEDGMENT

The support of the National Natural Science Foundation of China (Nos. 11372128 and 51175244) and National Safety Academic Foundation of China (No. U1730129) are gratefully acknowledged. The supports from the Collaborative Innovation Center of Advanced Aero-Engine, Jiangsu Province Key Laboratory of Aerospace Power System, the Key Laboratory of Aero-Engine Thermal Environment and Structure, Ministry of Industry and Information Technology are also gratefully acknowledged.

REFERENCES

[1] Ewins, D. J. 1973. Vibration characteristics of bladed disc assemblies. *J. of Mech. Eng. Science, 15*(3), 165-186.
[2] Pierre, C. 1988. Mode localization and eigenvalue loci veering phenomena in disordered structures. *J. of Sound & Vibration*, 126(3), 485-502.
[3] Ewins, D. J., 1991, ‘‘The Effects of Blade Mistuning on Vibration Response—A Survey,’’ IFToMM 4th International Conference on Rotordynamics, Prague, Czechoslovakia.
[4] Slater, J. S., Minkiewicz, G. R., and Blair, A. J., 1999, ‘‘Forced Response of Bladed Disk Assemblies—A Survey,’’ Shock Vib. Dig., Shock Vib. Dig., 31(1), pp. 17–24
[5] Castanier, M. P., & Pierre, C. 2006. Modeling and analysis of mistuned bladed disk vibration: current status and emerging directions. J. of Propulsion & Power, 22(2), 384-396.
[6] Whitehead, D. S. 1966. Effect of mistuning on the vibration of turbo-machine blades included by wakes. *J. of Mech. Eng. Science*, 8(1), 15-21.
[7] Whitehead, D. S. 1998. The maximum factor by which forced vibration of blades can increase due to mistuning. *J. of Eng. for Gas Turbines and Power-transactions of the ASME*. 120(1), 115-119.
[8] Martel, C. and Corral, R., 2009, Asymptotic description of maximum mistuning amplification of bladed disk forced response, *ASME J. of Eng. for Gas Turbines and Power.* Vol. 131, pp. 022506/1 – 022506/10
[9] Petrov, E. P., and Iglin, S. P., 1999, Search of the worst and best mistuning patterns for vibration amplitudes of bladed disks by the optimization methods using sensitivity coefficients, *Proc. of 1st ASSMO UK Conf. Eng. Design Optimization*, Ilkley, UK, pp. 303–310.
[10] Petrov, E. P., & Ewins, D. J. 2003. Analysis of the worst mistuning patterns in bladed disk assemblies. *ASME J. of Turbomachinery*, 125(4), 623-631.
[11] Rivas-Guerra, A.J., and Mignolet, M.P. 2003, “Maximum Amplification of Blade Response due to Mistuning: Localization and Mode Shapes Aspects of the Worst Disks,” J. of Turbomachinery, 125(3), pp. 442-454
[12] Kenyon, J.A., Griffin, J.H., Feiner, D.M., 2003, “Maximum Bladed Disk Forced Response from Distortion of a Structural Mode,” J. of Turbomachinery, 125(2), pp. 352-363.
[13] Han, Y., Xiao, B., Mignolet, M.P., “Expedient Estimation of the Maximum Amplification Factor in Damped Mistuned Bladed Disks,” Proc. ASME Turbo Expo 2007, Montreal, Canada, GT2007-27353
[14] Mignolet, M.P., Hu, W., and Jadic I., “On the Forced Response of Harmonically and Partially Mistuned Bladed Disks. Part I: Harmonic Mistuning; Part II: Partial Mistuning and Applications,,” Int. J. of Rotating Machinery, Vol. 6, No.1, pp. 29-56, 2000.
[15] Kenyon, J.A., and Griffin, J.H., 2003, ”Forced Response of Turbine Engine Bladed Disks and Sensitivity to Harmonic Mistuning,” Trans. ASME J. Eng. Gas Turbines Power 125(1), pp.113-120
[16] Nikolic, M., Petrov, E.P. and Ewins, D.J., “Robust strategies for forced response reduction of bladed discs based on large mistuning concept”, Trans. ASME: J. of Eng. for Gas Turbines and Power, 2008, Vol.130, March, 022501
[17] Jones, K.W., 2008, “Minimizing Maximum Modal Force in Mistuned Bladed Disk Forced Response”, J. of Turbomachinery, 130(1), 011011
[18] Rotea, M., and D’Amato, F., 2002, “New Tools for Analysis and Optimization of Mistuned Bladed Disks,”, 38th AIAA /ASME /SAE /ASEE Joint Propulsion Conference and Exhibit, July, AIAA 2002-4081
[19] Lalanne, B., 2005, “Perturbations Methods in Structural Dynamics and Applications to Cyclic Symmetric Domains,” Journal of Engineering for Gas Turbines and Power, 127, No. 3, pp. 654-662

[20] Petrov, E. P., Vitali, R., & Haftka, R. 2000. Optimization of mistuned bladed discs using gradient-based response surface approximations. *Proc. of the 41st AIAA/ASME/ASCE/AHS/ASC Struct., Struct. Dyn. and Materials Conf.* Vol.1, AIAA, Reston, VA, pp. 1129-1139.
[21] Duan, Y., Zang, C., & Petrov, E.P. 2016. Forced response analysis of high-mode vibrations for mistuned bladed disks with effective reduced-order models. *ASME J. of Eng. for Gas Turbines and Power*. 138(11).
[22] Petrov, E.P., Sanliturk, K. Y., & Ewins, D. J. 2002. A new method for dynamic analysis of mistuned bladed disks based on the exact relationship between tuned and mistuned systems. *ASME J. of Eng. for Gas Turbines & Power*, 124(3), 586-597.
[23] Chaoping Zang, Yuanqiu Tan, E.P. Petrov, "Analysis of Forced Response for Bladed Discs Mistuned by Material Anisotropy Orientation Scatters", *Trans. ASME J. Eng. Gas Turbines Power* 140(2), Feb. 2108, 022503
[24] Sinha, A., 2009, "Reduced-Order Model of a Bladed Rotor With Geometric Mistuning", *J. of Turbomachinery,* 131(3), 031007
[25] Nocedal, J., & Wright, S. 2006. Numerical optimization. *Springer Science & Business Media*.
[26] Mehrotra, S. 1992. On the implementation of a primal-dual interior point method. *SIAM J. on Optimization*, 2(4), 575-601.
[27] A. S. Nemirovski and M. J. Todd. 2009. Interior-point methods for optimization. *Acta Numerica,* pp. 1–44.
[28] Shultz, G. A., Schnabel, R. B., & Byrd, R. H. 1985. A family of trust-region-based algorithms for unconstrained minimization with strong global convergence properties. *SIAM J. on Numerical Analysis*, 22(1), 47-67.
[29] Byrd, R. H., Schnabel, R. B., & Shultz, G. A. 1988. Approximate solution of the trust region problem by minimization over two-dimensional subspaces. *Mathematical programming*, 40(1-3), 247-263.
[30] Boggs, P. T., & Tolle, J. W. 1995. Sequential quadratic programming. *Acta numerica*, 4, 1-51.
[31] Gould, N., Orban, D., & Toint, P. 2005. Numerical methods for large-scale nonlinear optimization. *Acta Numerica*, 14, 299-361.
[32] Byrd, R. H., & Waltz, R. A. 2011. An active-set algorithm for nonlinear programming using parametric linear programming. *Optimization Methods & Software*, 26(1), 47-66.
[33] Byrd, R. H., Gould, N. I., Nocedal, J., & Waltz, R. A. 2003. An algorithm for nonlinear optimization using linear programming and equality constrained subproblems. *Mathematical Programming*, 100(1), 27-48.